Available online at www.sciencedirect.com

ScienceDirect

Energy Procedia 92 (2016) 873 – 879

Energy Procedia

6th International Conference on Silicon Photovoltaics, SiliconPV 2016

Thermomechanical spalling of epitaxially grown silicon from porosified substrates

Verena Steckenreiter[a,]*, Jan Hensen[a], Alwina Knorr[a], Raphael Niepelt[a], Rolf Brendel[a,b], Sarah Kajari-Schröder[a]

[a]Institute for Solar Energy Research Hamelin (ISFH), Am Ohrberg 1, 31860 Emmerthal, Germany
[b]Department of Solar Energy, Institute of Solid-State Physics, Leibniz University of Hanover, Appelstraße 2, 30167 Hannover, Germany

Abstract

We combine two kerfless approaches to unite advantages of both processes: the epitaxial layer transfer based on porous silicon (PSI process) and the lift-off of a thin silicon layer from a substrate via controlled spalling by a stress-inducing layer. For this, we deposit an Al stressor layer on top of an epitaxially grown silicon layer. A porous double layer underneath the epitaxial layer serves as determined breaking point. We directionally heat this sample stack and cool it afterwards for controlled spalling of the epitaxial layer from the substrate. We achieve a lift-off rate of 34 out of 36 detached samples. The porous silicon layer enables a smooth surface of the detached epitaxial layer and the remaining substrate. Compared to our standard spalling process the thickness variation of the detached layers is significantly reduced from ≤ 25 μm to less than 2 μm. Furthermore we show that the lifetime of the detached epitaxial layers does not suffer from the Al deposition and the lift-off process.

Peer review by the scientific conference committee of SiliconPV 2016 under responsibility of PSE AG.

Keywords: kerf-free; layer transfer; spalling; exfoliation; stress-indusing layer; carrier lifetime

1. Introduction

Kerfless technologies offer the possibility to significantly reduce Si losses during wafer production. They can contribute to a further reduction of wafer production costs via (1) avoiding the standard kerf loss due to wafering, (2) by producing thinner Si wafers and (3) by eliminating processing costs for ingot growth and sawing. Several approaches were developed in recent years using porous Si [1,2], hydrogen implantation [3] or stressor layers [4] to

---

* Corresponding author. Tel.: +49-5151-999325; fax: +49-5151-999400.
E-mail address: v.steckenreiter@isfh.de

Peer review by the scientific conference committee of SiliconPV 2016 under responsibility of PSE AG.
doi:10.1016/j.egypro.2016.07.096

cleave thin Si layers. However, the thickness of the Si wafers is in general limited by handling issues during solar cell production. To overcome these handling limitations one can provide thin Si layers with an additional support layer. Therefore kerfless Si layers from the so-called porous silicon (PSI) process [1,2], which has the advantage of a well-defined breaking plane, were previously supported by ensapsulant/glass-stacks [5,6], backplanes [7], or thick polysilicon [8]. Finding the balance between non-detachability of the epitaxial layer and unintended lift-off of the same during front side processing requires effort, and a widening of the process window would be welcome for an enhanced process reliability. Another option to produce mechanically supported kerf-free thin Si layers is the spalling process [4]. Here a stress-inducing layer is deposited onto a silicon ingot or thick wafer. Due to thermo-mechanical stress during a temperature change a crack propagates parallel to the Si surface and exfoliates a thin layer from the substrate [4]. A metal stressor layer [9–12] can later function as a mechanical support and rear contact [13]. A potential advantage of the PSI process over spalling from compact silicon wafers [14] is a much smaller surface roughness.

In the present work we combine the advantages of both kerfless approaches: (1) the pre-determined separation layer in the form of porous Si controls the crack propagation, and (2) the stressor layer from the spalling process that mechanically supports the thin exfoliated Si layer and thus helps to avoid cracking of the thin Si layer during detachment. The use of a stressor layer expands the porous layer parameter window for successful lift-off.

2. Experimental

We prepare a porous double layer by electro-chemical etching in a solution consisting of HF, water, and the surfactant ethanol in volumetric relations of 1:1:1. A rim of 3 mm remains unporosified on the 6’’ substrate. By applying a step-wise current-profile we create a layer of low porosity on top, and a highly porous so-called separation layer underneath [15]. The separation layer is porosified with a current etch density in the range of 140 to 150 mA/cm^2. During reorganisation at a temperature of 1100°C in hydrogen atmosphere [16] the porous surface closes, resulting in a smooth surface allowing a low defect density [17] during subsequent epitaxial growth of a silicon layer on top [1]. The boron-doped epitaxial layer (0.5 Ωcm) has a thickness of 30 µm. We passivate the front side of the epitaxial layer by an 8 nm thick aluminium-oxide and 200 nm silicon-nitride stack.

The epitaxial layers used in this paper are not detachable by pure mechanical force due to enlarged Si bridges in the separation layer. We deposit a 30-µm thick Al layer in an inline evaporation system as a stressor layer for later lift-off [4]. Subsequently we heat the sample from the non-metalized side by a halogen lamp and immerge it directionally into a water bath [10]. The tensile stress in the metal layer induces the peeling of the epitaxial layer. Due to the directed heating and cooling of the sample there exists a temporary and spatial temperature variation across the substrate [10] that controls the crack propagation [18]. As expected, in doing so the porous silicon functions as determined breaking point. In case the epitaxial layer does not exfoliate completely (26 of 34 samples) it can then be easily be pulled off manually.

2.1. Lift-off

We prepare 36 samples as described above. We cut the samples out of 6’’ wafers after Al-deposition and choose three different geometries that are sketched in Fig. 1a): (I) 20 round samples with 5 cm in diameter, (II) 4 square samples with 5 cm edge length, and (III) 12 square samples of same size as (II) but with one corner cut off. Geometry (III) avoids the non-porosified edge at one of the four corners (II).

We completely separate 34 out of 36 samples. The two remaining layers break during exfoliation and about 5 to 6 mm^2 of the epitaxial layer remain on the substrate. The lift-off is successful at significantly reduced halogen lamp power setting when compared to previous exfoliations of Si layers without a PSI breaking layer: For successful lift-off we use a power per focus length of 15.0 to 19.3 W/cm. Niepelt et al. applied 34.2 W/cm for exfoliation in the same setup for non-porosified silicon samples [14] using the same apparatus.

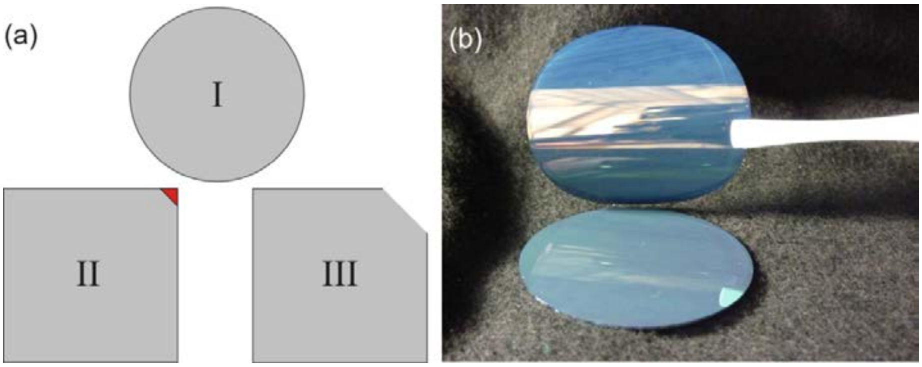

Fig. 1. (a) Schematic of the sample geometries. The red corner of sample geometry II marks the non-porosified area that is removed on sample geometry III; (b) Photograph of a detached epitaxial layer and its substrate with geometry (I). Both surfaces mirror the surrounding. Sample size is 5 cm in diameter.

Table 1 gives an overview of the exfoliation behavior of the 34 completely exfoliated samples and their visual appearance. From the 34 samples, 8 layers are completely separated from the substrate during the cooling process. In this case, the exfoliated layers remain in the water bath, and we collect them from there. Most of the layers, 26 at all, coil up partly during cooling. This means that the epitaxial layer exfoliates from the bottom of the sample on a distance of few mm to more than the half of the samples. It can be pulled off easily with a tweezer then, breaking the remaining Si pillars in the separation layer.

Table 1. Overview of the 34 successfully exfoliated samples and their visually defined status after exfoliation.

	No crack observable [no.]	Local crack observed [no.]
Complete exfoliation by directed cooling	4	4
Manually pulled off after directed cooling	21	5
Sum of samples	25	9

However, some samples show cracks after exfoliation. From the eight layers that fell off during immersion to the water bath we visually observe cracks in 4 samples, i.e. 50 % of the samples. Inspecting the 26 samples we have to pull off manually afterwards, only 5 samples show a crack. Thus, 19 % of the exfoliated samples are harmed.

The cracks are due to different sources: (1) The square-cut sample geometry II includes one corner without porous silicon. Due to the missing separation layer there, the epitaxial layer remains on the substrate, while the rest of the sample is completely exfoliated from the porous silicon area. In one case the non-detachability of the corner caused a crack that propagated into the detached epitaxial layer. (2) During exfoliation of another square-cut sample, the crack fronts start from three samples corners and meet in the centre. When pulling off the layer, it is folded and there a crack emerges. And (3), enlarged pillars in the separation layer lead to a crack formation in case of 7 samples, as observed visually. When applying the stress to the epitaxial layer it will start to exfoliate by breaking the pillars of the typical size (100-200 nm in diameter,) [19]. Then, at the enlarged pillar, no breakage occurs initially, but the stress builds up locally, finally leading to an abrupt breaking of the weakest spot, which may not be the pillar itself. Thus, cracks occur in the epitaxial layer.

While the sources (1) and (2) are eliminated by optimized sample geometry (III), thus avoiding the non-detachment at the non-porous rim, source (3) causes the most cracks. These cracks are small of about 1 to 5 mm length as visually observed. However, the crack formation due to porous silicon formation is independent on thermomechanical spalling or lift-off by mechanical force. However, the porous Si formation can be improved to avoid such issues.

2.2. Surface characteristics

It was already shown that a predetermined breaking plane leads to smoother surfaces after spalling [20]. Figure 1b) shows a photograph of a typical sample surface after lift-off as well as its parent substrate: the sample surface is visually flat. Figure 2 shows a profilometer scan that verifies the smoothness of the substrate. The maximum height variation at a scanning length of 35 mm is 1.7 µm. The total thickness variation of the substrate wafer is 1.00±0.34 µm prior to epitaxy. Hence, a height variation due to the porous silicon and / or the thermomechanical spalling is below 1 µm. With our standard spalling process without a predetermined breaking point we occasionally obtain up to factor 25 higher thickness variations in the samples centre. Furthermore, the defined breaking plane gives a homogeneous result above the whole sample as to see from Fig. 1b).

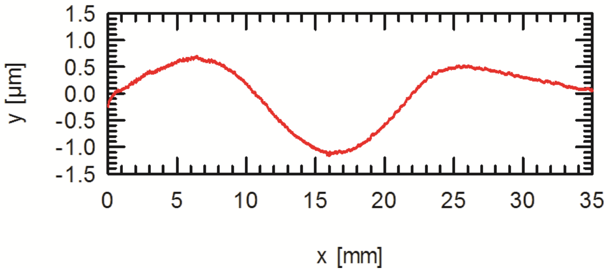

Fig. 2. Profilometer scan of a substrate wafer after exfoliation with residual porous silicon.

Figure 3 shows scanning electron microscope (SEM) micrographs of porous silicon that remains on the substrate after exfoliation of the epitaxial layer. Micrograph (a) shows the remaining porous Si from a mechanically non-detachable epitaxial layer, which contains a mixture of pillars and cavities. In micrograph (b) we observe a different structure, which has a well reorganized structure and allows the free standing detachment of a 9x9 cm^2 epitaxial layer. Single pillars have a diameter of about 120 nm or less. The structure of the separation layer (a) results in a low detachability of the epitaxial layer grown on top.

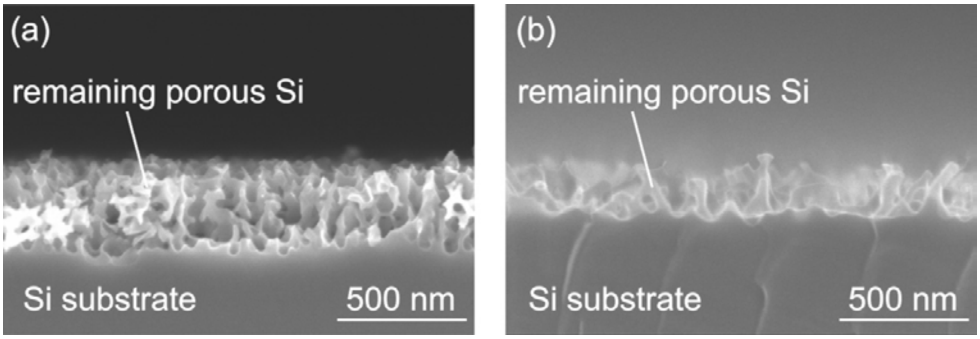

Fig. 3. SEM-micrographs of (a) remaining porous silicon on the substrate after cleavage of the epitaxial layer. The epitaxial layer was mechanically non-detachable. The here shown sample was cleaved during SEM sample preparation; (b) remaining porous silicon on the substrate after exfoliation of the epitaxial layer. The epitaxial layer was easily detachable and cleaved by mechanical force.

2.3. Silicon layer quality

Next we remove the Al and dielectric layer from the exfoliated epitaxial samples by etching in an HF solution to investigate the electronic properties of the exfoliated Si. After Al-removal the epitaxial layers flatten. We wet-chemically clean and passivate them with Al_2O_3. We then determine the carrier lifetime of these samples by quasi-steady state photoconductance decay measurements and find the charge carrier lifetime to be 32 to 36 μs at a minority carrier density of $\Delta n=10^{15}$ cm^{-3}. Epi layers from a similar batch but with weaker separation layers and that were detached without a stressor layer yielded about a factor 2 lower lifetime at same minority carrier density. Thus, the thermomechanical stress does not appear to harm the quality of the epitaxial layers at a lifetime level of 30 μs.

Figure 4 shows the local distribution of the lifetime. Lifetime mappings by microwave-photoconductance decay (MWPCD) method reveal locally varying lifetimes from 9 to 71 μs. As can be seen from Fig. 4 (a), the sample shows a lifetime above 40 μs in the centre and left bottom. Closer to the rim the carrier lifetime seems to be reduced. The lifetime distribution of the sample (b) shows a structure in form of two bows, whereby the ‘bows’ are of increased lifetime of up to 71 μs. In the bottom right we find spots of lower lifetime.

At this point, we cannot determine the reason of the inhomogeneous carrier lifetime distribution. A correlation with the exfoliation process is not apparent, as both samples from Figure 4 were exfoliated with exactly the same parameters. Nonetheless, we cannot definitely exclude the exfoliation process as the source of the lifetime inhomogeneity, although they may as well be due to the epitaxial growth, the reorganization process or the porous silicon removal.

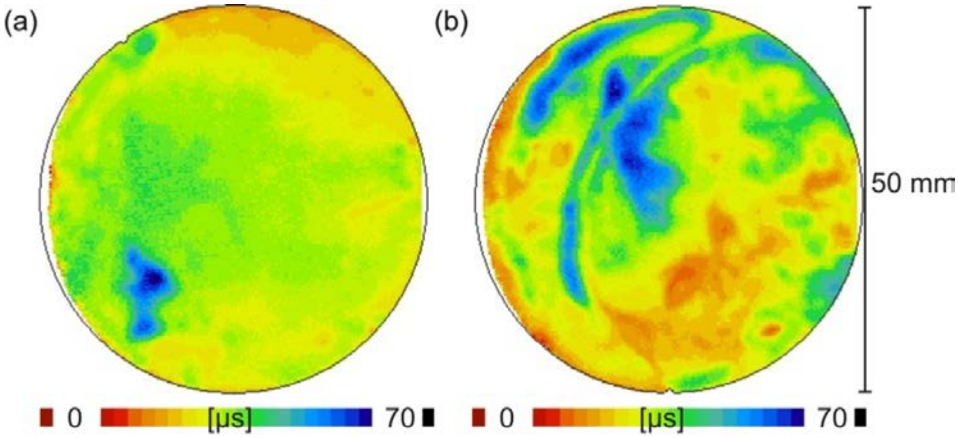

Fig. 4 (a) and (b). MWPCD mappings of two exfoliated epitaxial layers. After Al-removal the epitaxial layers are wet chemically cleaned and passivated by Al_2O_3.

4. Conclusion

The combination of spalling with the PSI process enables the lift-off of epitaxial layers that previously have not been detachable by pure mechanical force. Lifetime analysis as well as solar cell processing was not possible due to the non-accessibility of the rear side. We achieved a lift-off yield of 69 % crack-free samples with 36 samples in our first experiments.

Implementing a weak layer in the Si layer to exfoliate a monocrystalline Si layer by spalling requires additional processing efforts. However, the weak porous layer improves the layer smoothness compared to Si layers exfoliated from a compact Si wafer about a factor of 25. The layer quality as determined by QSSPC shows carrier lifetimes of 32 to 36 μs at $\Delta n=10^{15}$ cm^{-3} and on this level of comparable quality to other prepared batches. Spatially resolved

MWPCD mappings reveal some local inhomogeneities, which we currently cannot connect to the thermomechanical spalling process.

Due to porous Si formation that resulted in too large pillars in the separation layer, cracks can occur in the epitaxial layer during exfoliation. The cracking is not an inherent issue of the thermomechanical spalling and it can be mitigated by optimizing the porous double layer. At the same time the stressor layer mechanically supports the exfoliated thin Si layer.

The combination of the PSI-process with spalling extends the portfolio of controlled lift-off process and extends the processing window for successful lift off.

Acknowledgements

The authors thank Frank Heinemeyer for his valuable help with the sample metallization. We thank Dr. Felix Haase for support with lifetime data from epitaxial layers of a different batch. This work was supported by the Federal Ministry for Environment, Nature Conservation, and Nuclear Safety under the contract FKZ 0325461 and by the state of Lower Saxony.

References

[1] Brendel R. A novel process for ultrathin monocrystalline silicon solar cells on glass. In: 14th European Photovoltaic Solar Energy Conference; 1997. p. 1354–1358.
[2] Tayanaka H, Yamauchi K, Matsushita T. Thin-film crystalline silicon solar cells obtained by separation of a porous silicon sacrificial layer. In: 2nd World Conference and Exhibition on Photovoltaic Solar Energy Conversion; 1998. p. 1272–1277.
[3] Henley F, Lamm A, Kang S, Liu Z, Tian L. Direct Film Transfer (DFT) Technology for Kerf-free Silicon Wafering. In: 23rd European Photovoltaic Solar Energy Conference; 2008. p. 1090–1093.
[4] Tanielian M, Blackstone S, Lajos RE. A new technique of forming thin free standing single-crystal films. J. Electrochem. Soc. 1985;132:2507–09.
[5] Steckenreiter V, Horbelt R, Wright DN, Nese M, Brendel R. Qualification of encapsulation materials for module-level-processing. Solar Energy Materials and Solar Cells 2014;120396–401.
[6] Granata SN, Bearda T, Beaucarne G, Abdulraheem Y, Gordon I, Poortmans J, Mertens R. Silicone oxidation for a-Si:H passivation of wafers bonded to glass. Phys. Status Solidi RRL 2014;8:51–4.
[7] Kapur, P., Moslehi, M., Deshpande, A., Rana, V., Kramer, J., Seutter, S., Deshazer, H., Coutant, S., Calcaterra, A., Kommera, S., Su, Y.-S., Grupp, D., Tamilmani, S., Dutton, D., Stalcup, T., Du, T., Wingert, M. A Manufacturable, Non-Plated, Non-Ag Metallization Based 20.44% Efficient, 243cm2 Area, Back Contacted Solar Cell on 40um Thick Mono-Crystalline Silicon. In: 28th European Photovoltaic Solar Energy Conference and Exhibition; 2013. p. 2228–2231.
[8] Brendel R, Dullweber T, Gogolin R, Hannebauer H, Harder N, Hensen J, Kajari-Schröder S, Peibst R, Petermann JH, Römer U, Schmidt J, Schulte-Huxel H, Steckenreiter V. Recent progress and options for future crystalline silicon solar cells. In: 28th European Photovoltaic Solar Energy Conference and Exhibition; 2013. p. 676–691.
[9] Dross F, Robbelein J, Vandevelde B, van Kerschaver E, Gordon I, Beaucarne G, Poortmans J. Stress-induced large-area lift-off of crystalline Si films. Appl. Phys. A 2007;89:1149–52.
[10] Hensen J, Niepelt R, Kajari-Schroder S, Brendel R. Directional Heating and Cooling for Controlled Spalling. IEEE J. Photovoltaics 2015;5:1195–201.
[11] Bedell SW, Shahrjerdi D, Hekmatshoar B, Fogel K, Lauro PA, Ott JA, Sousa Cortes NE, Sadana D. Kerf-Less Removal of Si, Ge, and III–V Layers by Controlled Spalling to Enable Low-Cost PV Technologies. IEEE J. Photovoltaics 2012;2:2141–47.
[12] Rao RA, Mathew L, Saha S, Smith S, Sparkar D, Garcia R, Stout R, Gurmu A, Onyegam E, Ahn D, Xu D, Jawarani D, Fossum J, Banerjee S. A novel low cost 25μm thin exfoliated monocrystalline Si solar cell technology. In: Photovoltaic Specialists Conference (PVSC), 2011 37th IEEE.
[13] Niepelt R, Hensen J, Steckenreiter V, Brendel R, Kajari-Schröder S. Kerfless exfoliated thin crystalline Si wafers with Al metallization layers for solar cells. Journal of Materials Research 2015;30:213227–40.
[14] Niepelt R, Hensen J, Knorr A, Steckenreiter V, Kajari-Schroder S, Brendel R. High-quality exfoliated crystalline silicon foils for solar cell applications. Energy Procedia 2014;55570–77.
[15] Brendel R, Auer R, Artmann H. Textured Monocrystalline Thin-Film Si Cells from the Porous Silicon (PSI) Process. Prog. Photovolt: Res. Appl. 2001;217–21.
[16] Labunov V, Bondarenko V, Glinenko I, Dorofeev A, Tabulina L. Heat treatment effect on porous silicon. Thin Solid Films 1986;137:1123–34.
[17] Sato N, Sakaguchi K, Yamagata K, Fujiyama Y, Nakayama J, Yonehara T. Advanced Quality in Epitaxial Layer Transfer by Bond and Etch-back of Porous Si. Jpn. J. Appl. Phys. 1996;35:2B973–77.

[18] Berardone I, Kajari-Schröder S, Niepelt R, Hensen J, Steckenreiter V, Paggi M. Numerical modelling and validation of thermally-induced spalling. Energy Procedia 2015;77855–62.

[19] Kajari-Schröder S, Käsewieter J, Hensen J, Brendel R. Lift-off of Free-standing Layers in the Kerfless Porous Silicon Process. Energy Procedia 2013;38919–25.

[20] Siltectra zeigt Cold Split Prozess auf 200mm Siliziumwafer; 2014. Available from: http://www.siltectra.com/siltectra-zeigt-cold-split-prozess-auf-200mm-siliziumwafer/.